Supporting Information

Tetrathiafulvalene-based Nanotweezers – Non-covalent Binding of Carbon Nanotubes in Aqueous Media with Charge Transfer Implications

Carlos Romero-Nieto,[†] Raúl García,[‡] M. Ángeles Herranz,[‡] Christian Ehli,[†] Michaela Ruppert,[§] Andreas Hirsch,*[,§] Dirk M. Guldi,*[,†] and Nazario Martín*[,‡,¥]

[†] Department of Chemistry and Pharmacy & Interdisciplinary Center for Molecular Materials (ICMM), Friedrich-Alexander-Universität Erlangen-Nürnberg, Egerlandstrasse 3, 91058 Erlangen, Germany

[‡] Departamento de Química Orgánica, Facultad de Química, Universidad Complutense de Madrid, 28040 Madrid, Spain

[§] Department of Chemistry and Pharmacy, Friedrich-Alexander-Universität Erlangen-Nürnberg, Henkestrasse 42, 91054 Erlangen, Germany

[¥] IMDEA-Nanoscience, Campus de Cantoblanco, 28049 Madrid, Spain

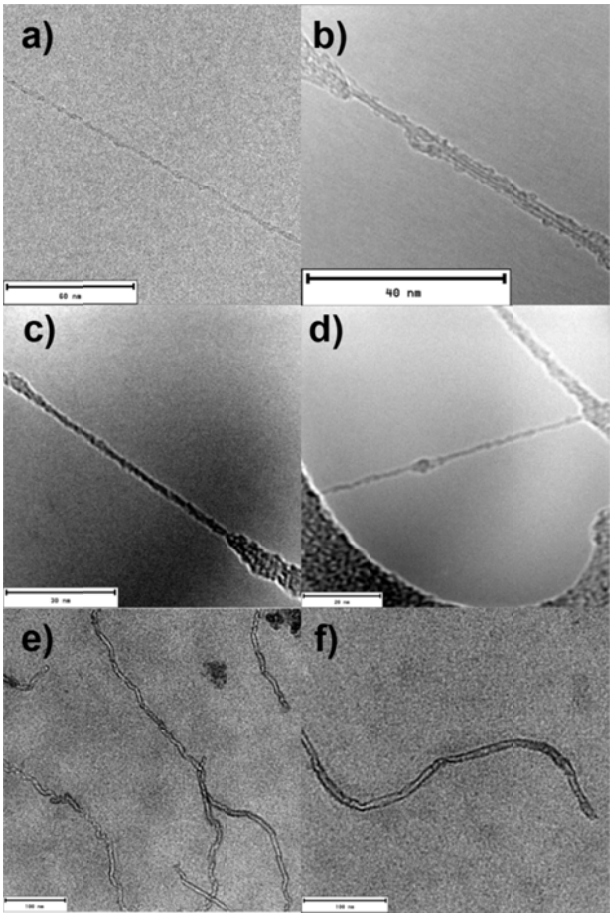

Figure S1. a) and b) Representative TEM images of HiPco SWCNT/SDBS on holey carbon grids with scale bars of 60 and 40 nm, respectively. c) and d) Representative TEM images of CoMoCAT SWCNT/SDBS on holey carbon grids with scale bars of 30 and 20 nm, respectively. e) and f) Representative TEM images of MWCNT/SDBS on standard formvar film coated copper grids with scale bars of 100 nm.

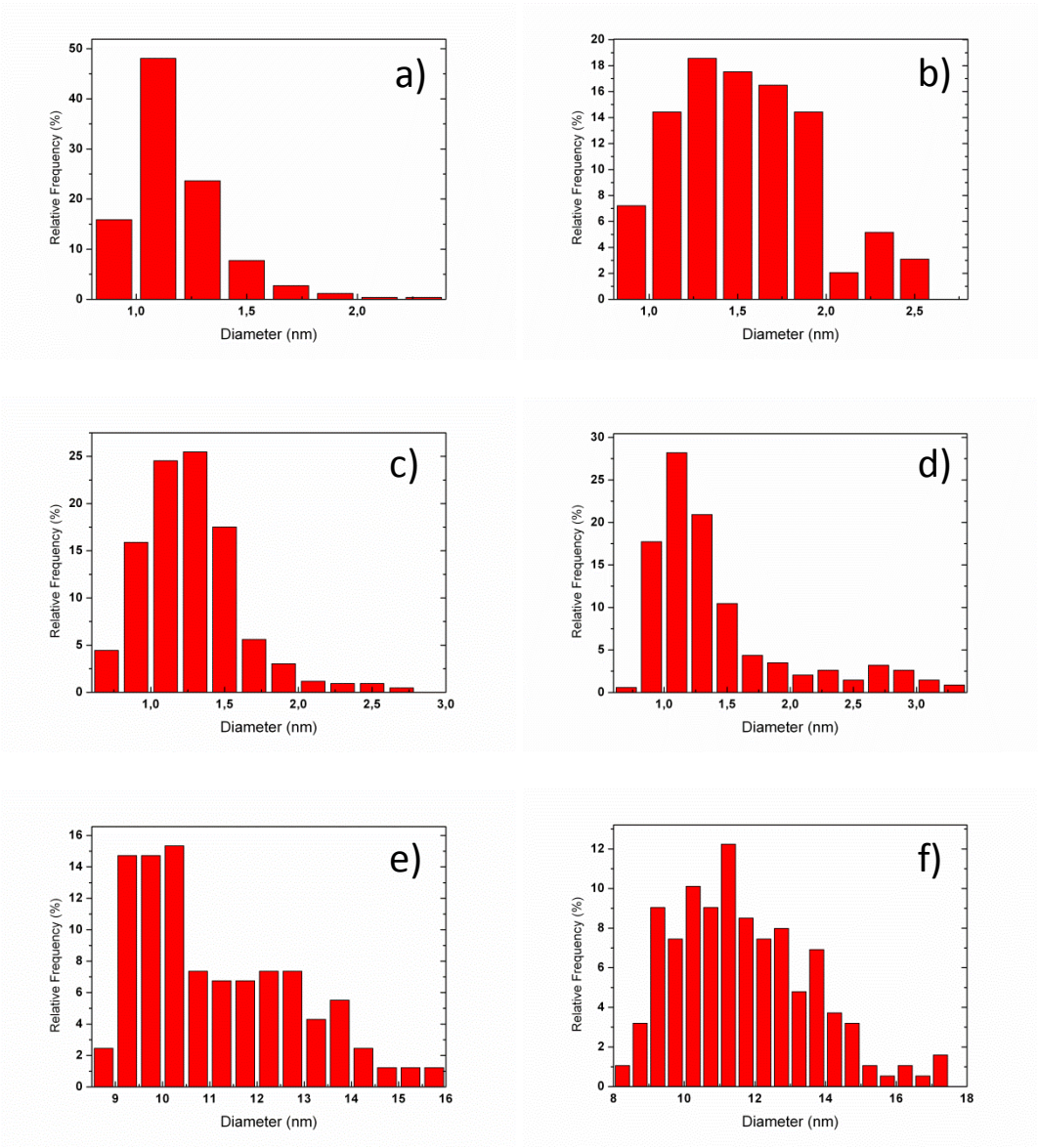

Figure S2. Diameter distributions based on TEM investigation – see, for example, Figures 2 and S1 – of a) HiPco SWCNT/SDBS with a mean diameter of 1.18 nm, b) HiPco SWCNT/**8** with a mean diameter of 1.54 nm, c) CoMoCAT SWCNT/SDBS with a mean diameter of 1.27 nm, d) CoMoCAT SWCNT/**8** with a mean diameter of 1.43 nm, e) MWCNT/SDBS, with a mean diameter of 11.14 nm, and MWCNT/**8** with a mean diameter of 11.64 nm.

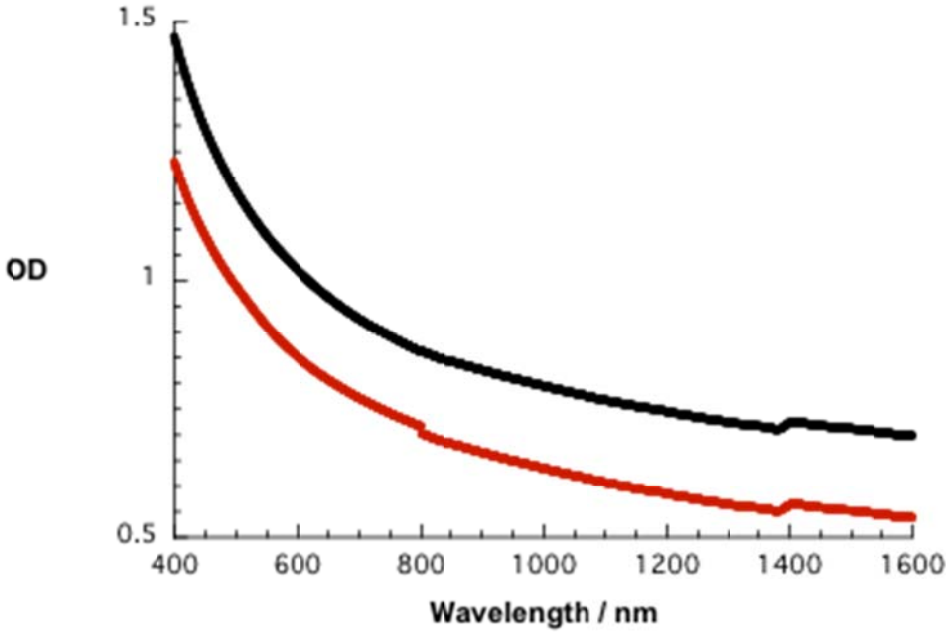

Figure S3. Absorption spectra of MWNT/SDBS (red spectrum) and of MWNT/**8** (black spectrum) in D_2O.

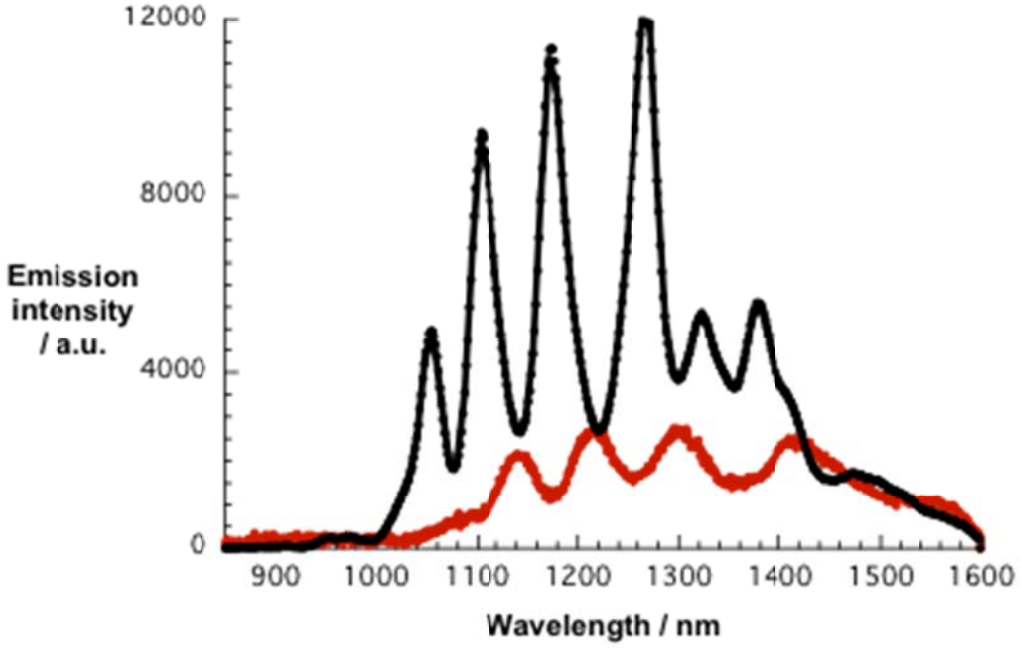

Figure S4. Comparison of the NIR fluorescence spectra of HiPco SWCNT/SDBS (black spectrum) and HiPco SWCNT/**8** (red spectrum) amplified by a factor of 5 in D_2O excitation at 651 nm.

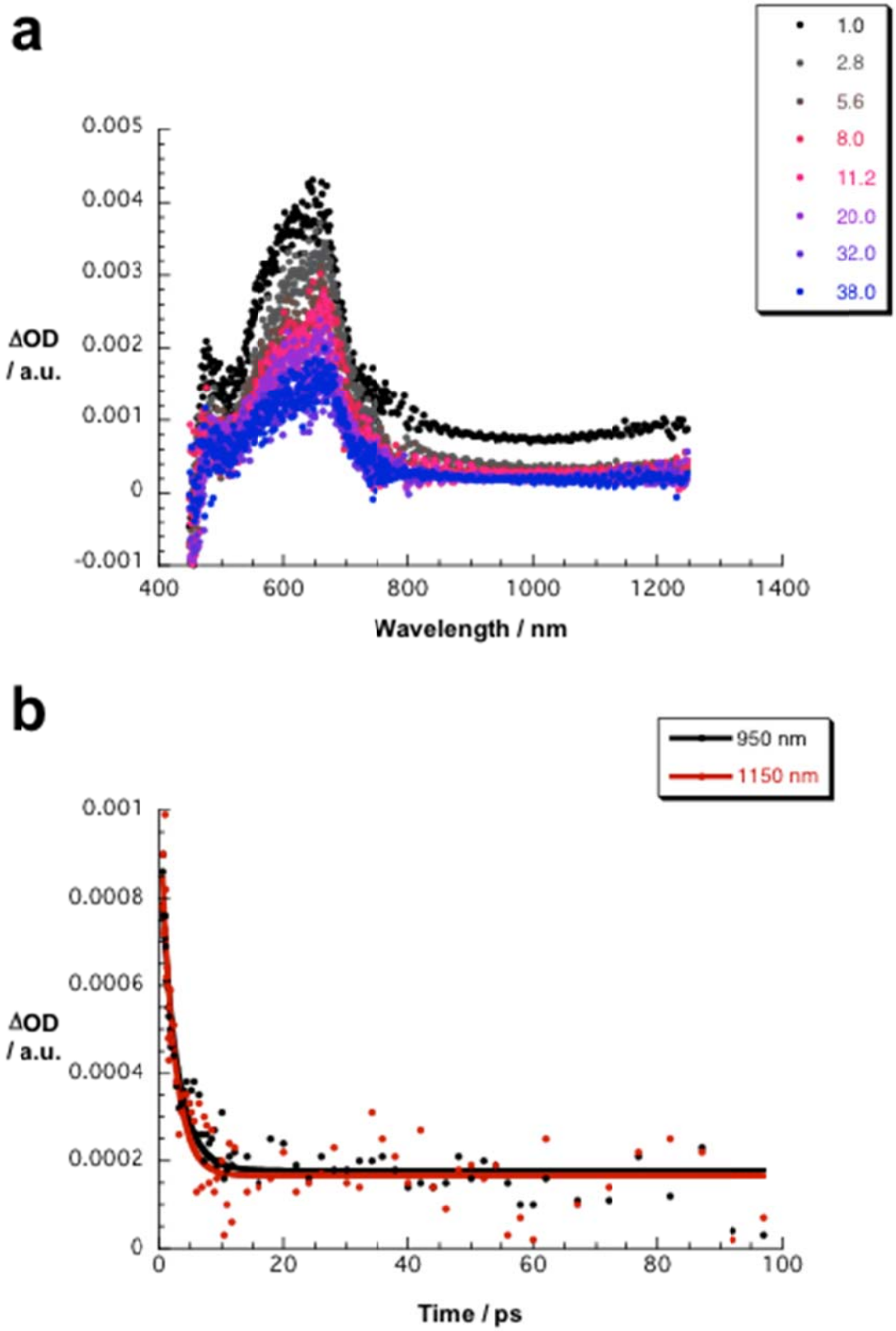

Figure S5. a) Differential absorption spectra (visible and near-infrared) obtained upon femtosecond pump probe experiments (387 nm) of **8** in D_2O with several time delays between 0 and 38 ps at room temperature. b) Time absorption profiles of the spectra shown above at 950 and 1150 nm monitoring the excited state decay.

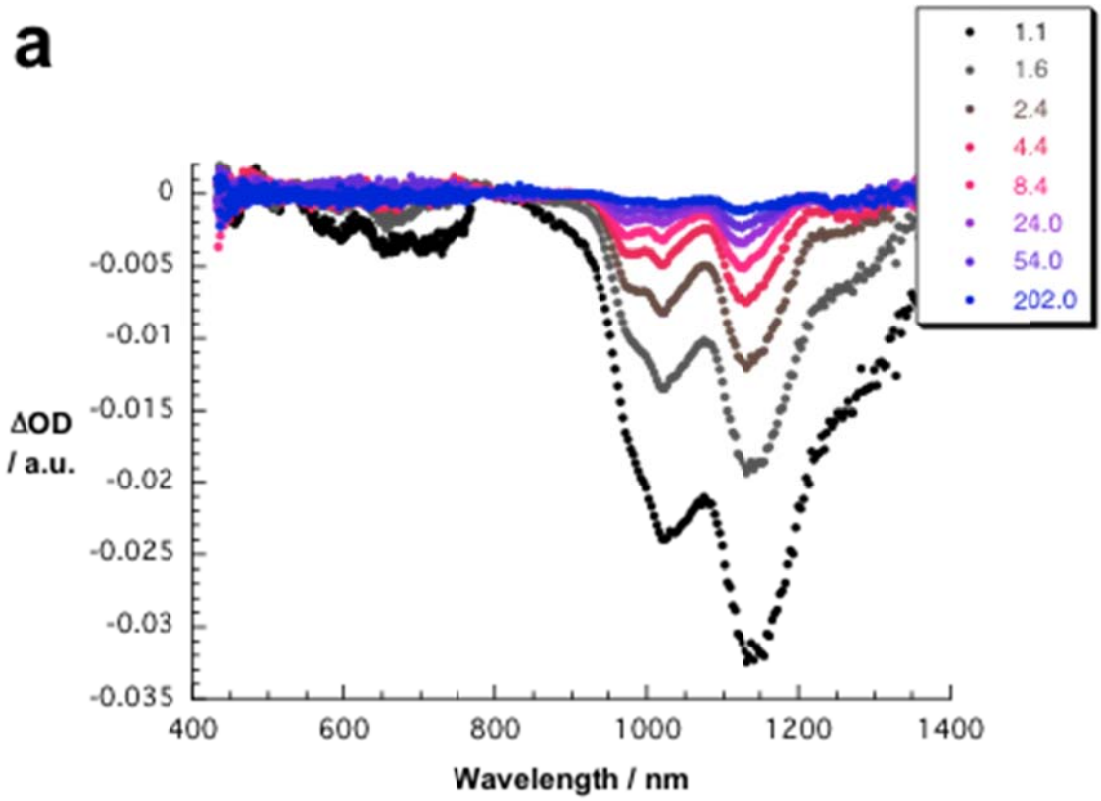

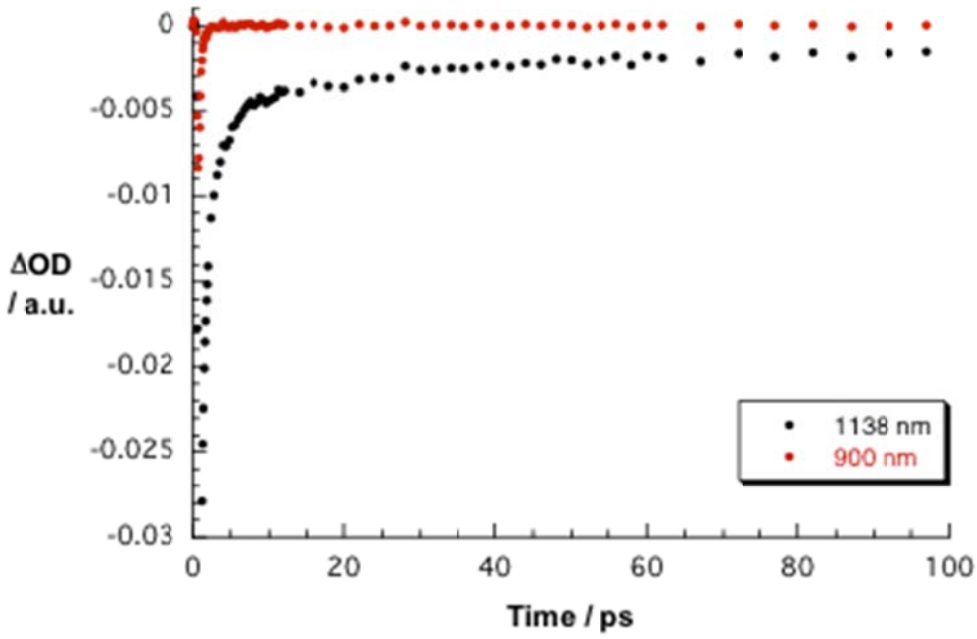

Figure S6. Upper part – differential absorption spectra (visible and near-infrared) obtained upon femtosecond pump probe experiments (387 nm) of HiPco SWCNT/SDBS in D_2O with several time delays between 0 and 28 ps at room temperature. Lower part – time absorption profiles of the spectra shown above at 950 and 1160 nm monitoring the excited state decay.

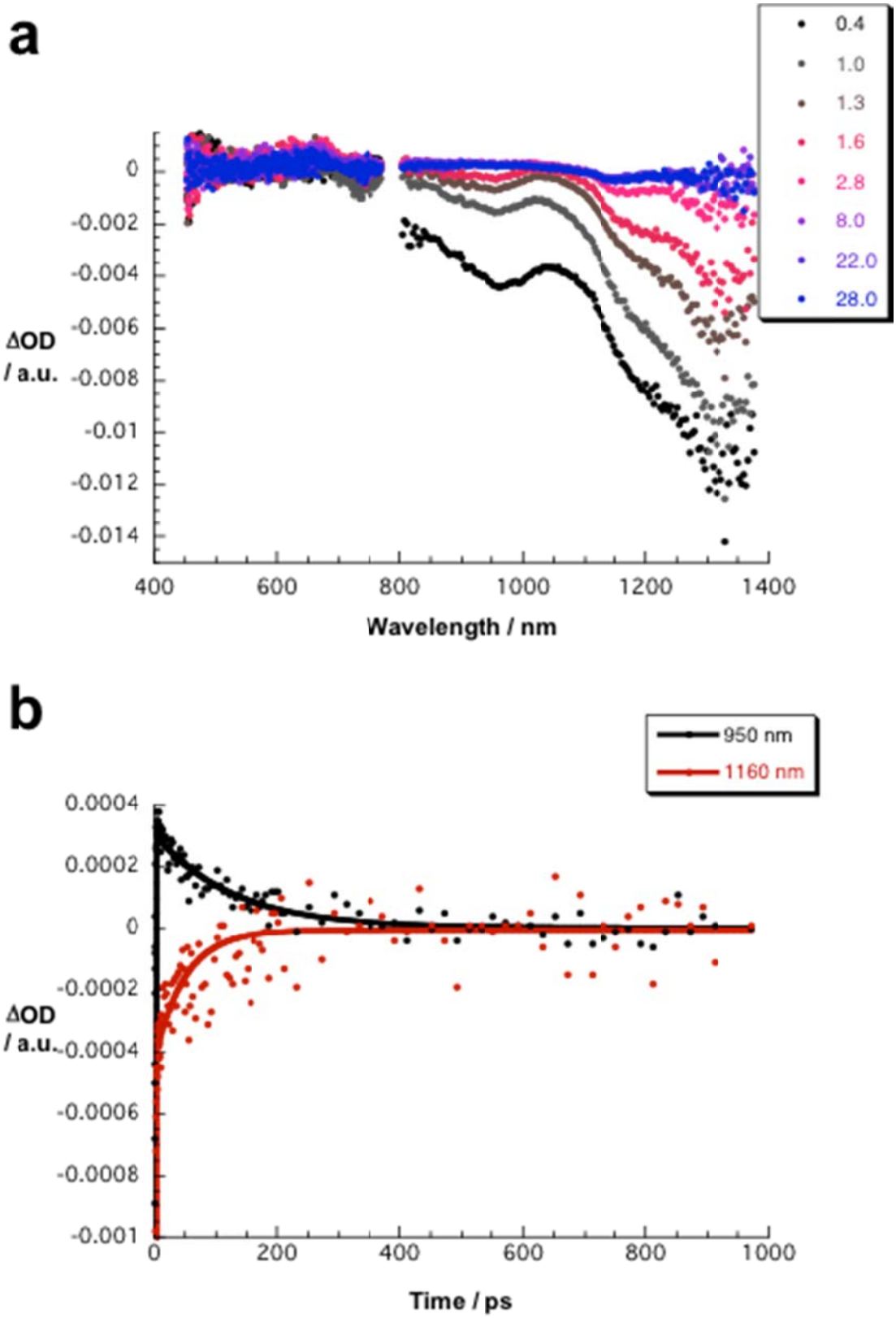

Figure S7. a) Differential absorption spectra (visible and near-infrared) obtained upon femtosecond pump probe experiments (387 nm) of HiPco SWCNT/**8** in D_2O with several time delays between 0 and 28 ps at room temperature. b) Time absorption profiles of the spectra shown above at 950 and 1160 nm monitoring the excited state decay.

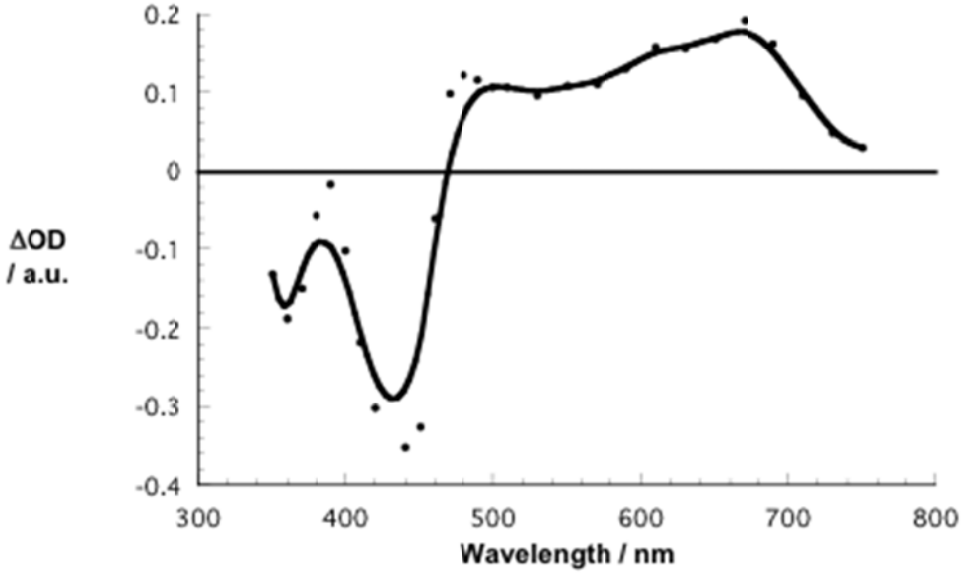

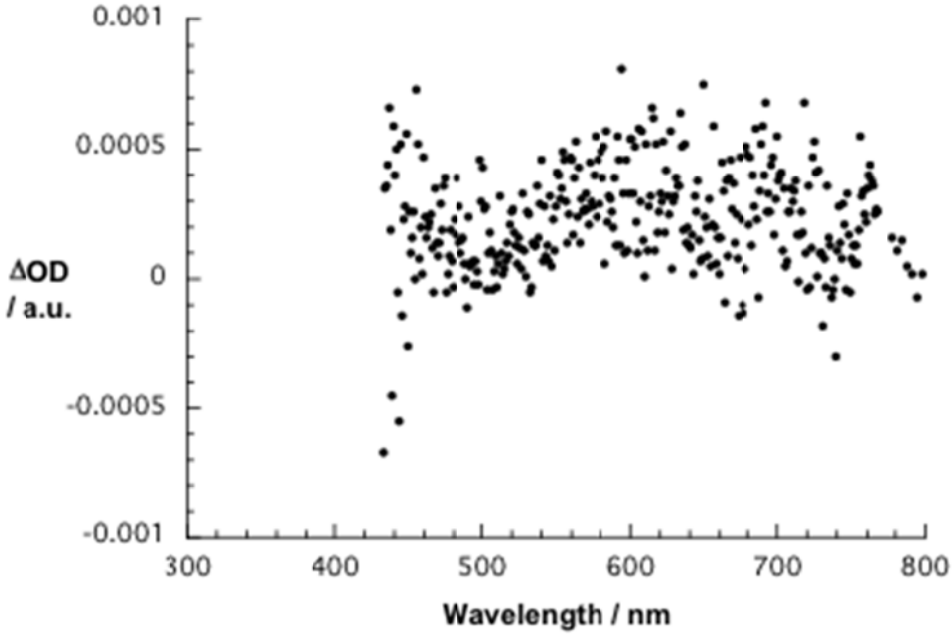

Figure S8. Upper part – differential absorption spectrum (visible and near-infrared) obtained upon pulse radiolytic oxidation of exTTF in oxygenated dichloromethane solutions 200 µs after the pulse. Lower part – differential absorption spectrum (visible and near-infrared) obtained upon femtosecond pump probe experiments (387 nm) of CoMoCAT SWCNT/**8** in D_2O with a time delay of 14 ps at room temperature.

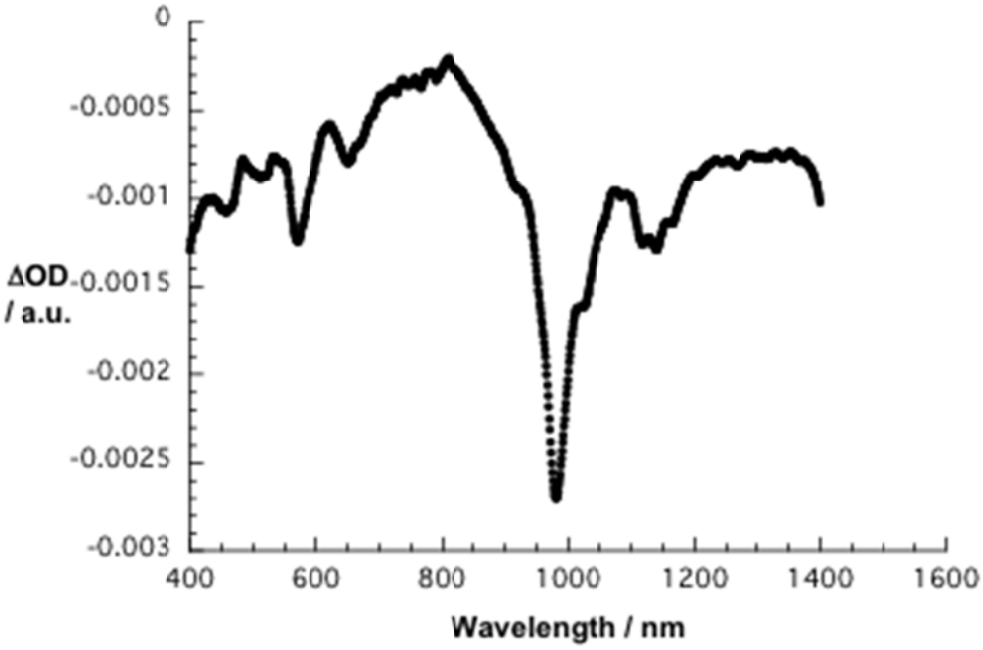

Figure S9. Differential absorption spectrum (visible and near-infrared) obtained upon electrochemical reduction of CoMoCAT SWCNT/SDBS in D_2O with applied voltages of -0.8 V (black spectrum) at room temperature.